RAPID COMMUNICATIONS

PHYSICAL REVIEW B VOLUME 39, NUMBER 9 15 MARCH 1989-II

# Quantum Hall effect in wide parabolic GaAs/$Al_xGa_{1-x}As$ wells

E. G. Gwinn, R. M. Westervelt, P. F. Hopkins, and A. J. Rimberg
*Division of Applied Sciences and Department of Physics, Harvard University, Cambridge, Massachusetts 02138*

M. Sundaram and A. C. Gossard
*Department of Electrical and Materials Engineering and Materials Department, University of California at Santa Barbara, Santa Barbara, California 93106*

(Received 8 September 1988; revised manuscript received 15 November 1988)

Parabolic GaAs/$Al_xGa_{1-x}As$ wells are used to create thick (> 1000 Å) spatially uniform layers of electron gas with low-temperature mobility $\mu=(0.2\text{–}2.5)\times10^5$ cm$^2$/V sec. Measurements of the integer quantum Hall effect in a 4000-Å-wide parabolic well as the well is partially filled with electrons are used to study the transition from two-dimensional toward three-dimensional behavior.

A three-dimensional electron gas in a strong magnetic field at low temperatures is predicted to show interesting phenomena when the electronic charge is canceled by a uniform positive background. These include the quantum Hall effect[1,2] and possible collective electronic states.[3] Because electrons in doped semiconductors interact strongly with the background of positive point charges, producing magnetic freeze-out, unambiguous experimental tests of these predictions have been difficult to make.[3]

Remotely doped parabolic GaAs/$Al_xGa_{1-x}As$ wells can be used to create relatively thick (> 1000 Å) layers of electron gas[3–7] with low-temperature mobility as high as[5] $\mu=2.5\times10^5$ cm$^2$/V sec, which do not freeze-out in strong magnetic fields.[5] These structures show both the integer[5–7] and fractional[5] quantum Hall effect. In this paper we report magnetotransport measurements on a 4000-Å-wide parabolic well as it is partially filled with electrons using persistent photoconductivity. The data show that the well fills at constant Fermi energy via an increase in width as expected for a spatially uniform slab of constant density, and they show how the integer quantum Hall effect changes in the transition away from two dimensions as the slab becomes thicker.

Figure 1 illustrates the conduction-band edge versus position for empty and partially filled parabolic wells.[4] For the empty well in Fig. 1(a) the parabolic potential of depth $\Delta_1$ is confined by a barrier of height $\Delta_2$. Remotely located dopant layers on both sides are used to fill the well with electrons. The parabolic potential in Fig. 1(a) is identical to that produced by a three-dimensional (3D) spatially uniform slab of positive charge of density $n_+=2\varepsilon\Delta_1/\pi e^2w^2$. The electrons act to screen this fictitious charge as they enter the well. When the well is full, the electron density $n$ is constant and equal to $n_+$ in the limit that many electric subbands are occupied. The total self-consistent potential is then just that of a square well of width $w$ and depth $\Delta_2$. Even when the well is partially full, as in Fig. 1(b), the electrons screen the parabolic potential and create a thinner slab of comparable density $n\simeq n_+$ over part of the width $w_e$ as indicated. As the well fills with electrons, the width $w_e$ of the electron layer increases while the density and the Fermi energy $E_F$ remain approximately constant. This process does not require precise control of the doping to create spatially uniform electron density profiles, although precise control over the parabolic profile is necessary. These concepts can be generalized[4] to create density profiles other than those in Fig. 1.

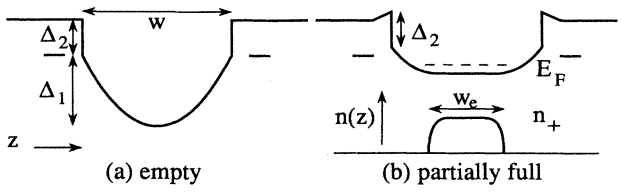


FIG. 1. Schematic illustration of the conduction-band edge vs position for a parabolic well (see text).

It is also interesting to consider the filling of a parabolic well when the number of occupied subbands is not large, as for the experiments presented here. For a wide well partially filled with a dense electron gas, the electrostatic energy is typically much larger than the kinetic energy ($\Delta_1=150$ meV, and $E_F=2.8$ meV for the data below). The electronic wave functions $\psi_i(z)$ thus tend to flatten at the expense of additional kinetic energy in order to produce a more uniform charge distribution and reduce the pseudoelectrostatic energy. For example, $n(z)$ in Fig. 1(b) could also illustrate the spatial profile of the charge density when only one subband is occupied. As for the semiclassical case, this process does not depend critically on doping, and can be used to produce other wavefunction profiles.

The energy spectrum $E_j$ of a partially filled parabolic well roughly approximates that of a square well $E_{Sj}=j^2E_0$ of width $w_e$ equal to that of the electron layer, with $E_0=(h/w_e)^2/8m_e$ and $m_e=0.067m_0$. However, when only a few subbands are occupied, their energies are shifted upward due to the increased kinetic energy associated with bending and flattening of the wave function. When more than one subband is occupied, filling of the well is expected to occur at approximately constant Fermi

 

energy $E_F - E_1$, corresponding to constant density, while the separation between two given subbands decreases as the electron layer becomes wider. The number of occupied subbands increases while the Fermi energy remains approximately constant.

We have studied five parabolic well structures with low-temperature Hall mobilities between $\mu_H = 2\times10^4$ cm$^2$/Vsec and $\mu_H = 2.5\times10^5$ cm$^2$/Vsec, and with widths from $w = 1000$ to 4000 Å. We present data here for a 4000-Å well with $\mu_H = 5\times10^4$ cm$^2$/Vsec and design parameters $\Delta_1 = 150$ meV (for which $n_+w = 2.2\times10^{11}$ cm$^2$) and $\Delta_2 = 75$ meV. These structures were grown[4] using molecular beam epitaxy on semi-insulating GaAs substrates. The parabolic potential was created by changing the relative thickness of alternating GaAs and $Al_{0.3}Ga_{0.7}As$ layers in a fine superlattice of period 20 Å so that the average Al concentration varied parabolically from $x = 0$ in the center to $x = 0.2$ at the edge of the well. Electrons were deposited in the well from Si-doped layers symmetrically set back 200 Å from both sides of the well in the $Al_{0.3}Ga_{0.7}As$ barrier.

Photolithographically defined Hall bars with dimensions $0.5\times5$ mm$^2$ were prepared with In electrical contacts, produced by baking for 5 min at 400 °C in a reducing atmosphere. The samples were mounted stress free and cooled slowly in the dark in a dilution refrigerator equipped with a 7-T superconducting solenoid. Measurements of the transverse Hall and magnetoresistance $R_{xy}$ and $R_{xx}$ with the magnetic field perpendicular to the plane of the sample, and the longitudinal magnetoresistance $R_L$ with an in-plane magnetic field, were made using lock-in techniques and recorded in a computer; typical values of the applied current were $I \sim 30$ nA. Between the transverse and longitudinal data sets below, the sample was warmed to room temperature for remounting. The measured low-temperature areal Hall density was $n_H = 0.78\times10^{11}$ cm$^2$ before illumination, indicating that the well

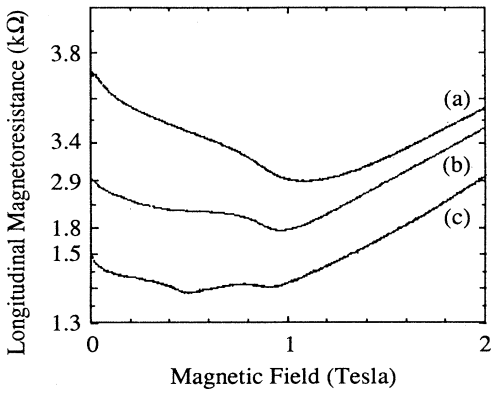


FIG. 3. Longitudinal magnetoresistance: (a) before illumination, zero-field resistance $R_0 = 3650$ Ω; after illumination: (b) $R_0 = 2050$ Ω, (c) $R_0 = 1500$ Ω.

was roughly $\frac{1}{3}$ full as grown with $n_H/n_+w = 0.36$. Electrons were added to the well by illuminating the sample *in situ* in zero magnetic field with a light-emitting diode.

Measurements of the longitudinal magnetoresistance $R_L$ with the magnetic field in the plane of the sample and parallel to the current direction were used to determine the number of occupied subbands as previously done for doped square wells.[8] Figure 2 illustrates the magnetic field dependence of the bottoms $E_j$ of the subbands of a square well with an in-plane magnetic field $H$, for two different energy-level separations, adjusted to fit the data shown in Figs. 3–5. The energies $E_j$ smoothly change from the energy levels of a square well $E_{Sj} = j^2(h/w_e)^2/8m_e$ to the corresponding levels of a Landau fan $E_{Hj} = [(j-1)+\frac{1}{2}]\hbar\omega_c/2\pi$ as $H$ increases.[8] For purposes of illustration, the interpolation formula $E_j = (E_{Sj}^2 + E_{Hj}^2)^{1/2}$ is shown in Fig. 2; numerical calculations[8] for square wells yield similar results for $E_j$. Transverse Shubnikov–de Haas measurements for low magnetic

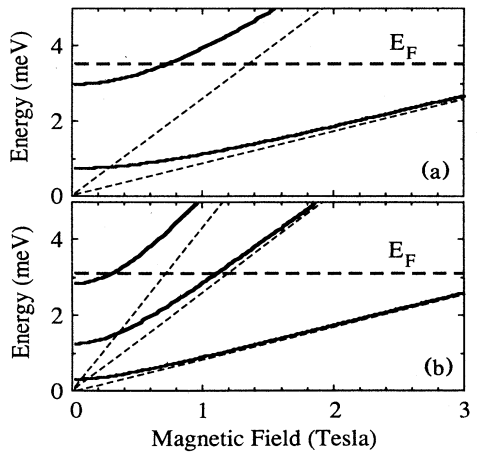


FIG. 2. Longitudinal subband energies vs magnetic field for square wells of increasing thickness: (a) $E_2 - E_1 = 2.25$ meV, (b) $E_2 - E_1 = 0.95$ meV. The zero-field Fermi energy $E_F - E_1 = 2.8$ meV is indicated in both (a) and (b); the field-dependent Fermi energy oscillates about this value.

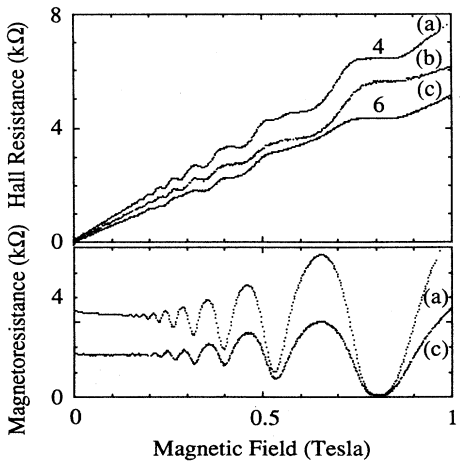


FIG. 4. Transverse Hall and magnetoresistance: (a) before illumination, $R_0 = 3540$ Ω; after illumination: (b) $R_0 = 2120$ Ω, (c) $R_0 = 1800$ Ω.

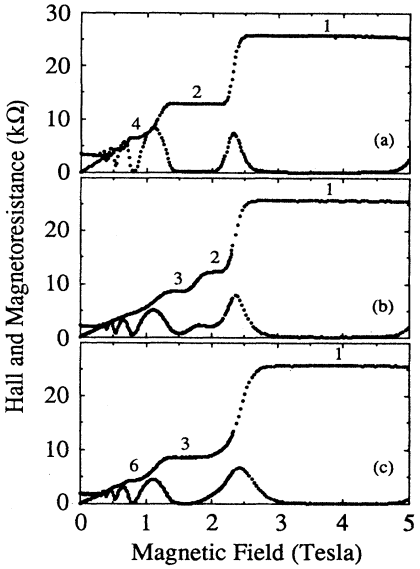


FIG. 5. Transverse Hall and magnetoresistance: (a) before illumination, $R_0=3540\ \Omega$; after illumination: (b) $R_0=2120\ \Omega$, (c) $R_0=1800\ \Omega$.

fields (see Fig. 4) show that the Fermi energy $E_F-E_1=2.8$ meV in zero field remains nearly constant as the well is filled; this zero-field value is shown as the bold dashed line in Figs. 2(a) and 2(b) (see caption). Following Yoshino, Sakaki, and Hotta,[8] we associate each peak in $R_L$ with a crossing between $E_F$ and the bottom of a subband $E_j$ with $j>1$. The use of another point on the oscillation does not qualitatively change our conclusions.

Longitudinal magnetoresistance data taken at $T=50$ mK are shown in Fig. 3(a) before illumination, and in Figs. 3(b) and 3(c) after increasing periods of illumination. The data before illumination in Fig. 3(a) show a single peak in $R_L$ near $H=0.7$ T indicating the transition from two occupied subbands to one, as illustrated in Fig. 2(a). As electrons are added to the well in Figs. 3(b) and 3(c), this peak moves relatively little as expected for constant Fermi energy, and a new peak is introduced at lower fields corresponding to the transition from three to two occupied subbands [Fig. 2(b)]. These data demonstrate that two subbands of the well are occupied as grown, and confirm that a parabolic well fills with electrons by decreasing the separation of the subbands.

Figures 4 and 5 present measurements of the transverse Hall and magnetoresistance $R_{xy}$ and $R_{xx}$ at $T=50$ mK after increasing periods of illumination approximately corresponding to the range in Figs. 3(a) to 3(c), based on the resistance $R_0$ in zero magnetic field. The Shubnikov-de Haas oscillations in $R_{xx}$ shown in Fig. 4 show that the zero-field Fermi energy $E_F-E_1=2.8\pm0.1$ meV remains essentially constant as electrons are added to the well, while the zero-field resistance drops by a factor $\sim2$ and the number of occupied subbands increases from 2 to 3 (from Fig. 3). This Fermi energy is somewhat larger than one would naively expect for a square well of width $w_e\sim n_H/n_+\sim1500$ Å corresponding to the measured Hall density ($E_F-E_1\sim1.8$ meV); however, a full self-consistent calculation of the energy levels is needed to make a quantitative comparison. The low-field Hall resistance $R_{xy}$ in Figs. 4(a) to 4(c) decreases continuously with illumination and exhibits quantum-Hall-effect steps. The measured areal Hall density $n_H$ increased with illumination from $n_H=0.78\times10^{11}$ cm$^{-2}$ to $n_H=1.12\times10^{11}$ cm$^{-2}$ over the range shown in Figs. 4(a) to 4(c). Note that $n_H$ can underestimate the true areal density when more than one subband is occupied.[9]

Figures 4 and 5 display well-developed quantum-Hall plateaus $R_{xy}=h/ve^2$ at integer filling factors $\nu$. The magnetoresistance $R_{xx}$ approaches zero at Hall steps both before and after illumination, evidence against the possible formation of parallel conduction paths. A plot of the Landau levels for the transverse case neglecting spin splitting is shown for comparison in Figs. 6(a) and 6(b) to help clarify the following discussion; spin splitting is experimentally important as discussed below. The electric subband energies and the zero-field Fermi energy $E_F-E_1$ shown are the same as for Figs. 2(a) and 2(b), respectively, and they correspond approximately to the range of illumination for the transverse data. Whenever the Fermi energy lies in band of localized states between Landau levels, a quantum Hall step will occur with filling factor $\nu$ equal to the number of spin-split Landau levels below $E_F$, according to conventional theory.[1]

Figures 4 and 5 demonstrate how the quantum Hall effect changes in the transition from two dimensions toward three dimensions as the electron layer becomes thicker and more subbands are occupied. Before illumination in Fig. 5(a), well-developed Hall plateaus are seen in the data for $\nu=1$, 2, and 4. As shown in Fig. 6(a), the second subband, occupied at $H=0$ [Figs. 3(a)], empties at a transverse field below that for the $\nu=4$ step at $H=0.8$ T, and thus the observed quantum Hall effect in Figs. 4(a) and 5(a) is two dimensional, with only the lowest electric subband occupied. As more electrons are added to the well, the thickness $w_e$ of the electron layer increases, and

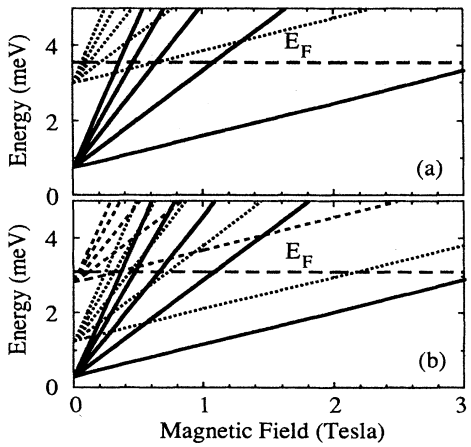


FIG. 6. Transverse Landau levels for square wells of increasing thickness: (a) $E_2-E_1=2.25$ meV and (b) $E_2-E_1=0.95$ meV. The zero-field Fermi energy $E_F-E_1=2.8$ meV is indicated in both (a) and (b); the field-dependent Fermi energy oscillates about this value.

the separation of the subband energies at $H=0$ decreases introducing a third subband beneath the Fermi energy [Fig. 3(c)], as in Fig. 6(b). With more than one subband occupied, the filling factor of Hall steps in $R_{xy}$ increase, while the corresponding minima in $R_{xx}$ remain near the same magnetic fields. As electrons are added to the well in Figs. 4(a) to 4(c) and in Figs. 5(a) to 5(c), the $\nu=4$ step first disappears, then reappears as a $\nu=6$ step at the same magnetic field, due to the introduction of an unsplit Landau level from the second subband beneath the Fermi energy (Fig. 6). Over the same range of illumination in Figs. 5(a) to 5(c), an additional Hall step appears at $\nu=3$, and the steps at $\nu=2$ weakens and disappears. After additional illumination the $\nu=2$ step reappears at a higher field, $H=2.5$ T. Comparison of this data with Fig. 6(b) suggests that these changes are caused by the introduction of a spin-split Landau level from the second subband below the Fermi level. The absence of the $\nu=2$ step in Fig. 3(c) is presumably due to an accidental degeneracy between the upper spin level of the first subband and the lowest spin level of the second subband.

In conclusion, we have shown that parabolic wells can be used to create relatively thick layers of high-mobility electron gas, which fill with electrons at essentially constant Fermi energy via an increase in width. Magnetoresistance and Hall effect data taken as electrons are added to the well show how the integer quantum Hall effect makes the transition from two dimensions towards three dimensions. The magnetic field of integer steps remains fixed as electrons are added to the well because the Fermi energy remains unchanged, while the filling factors increase with thickness of the electron layer. In the conventional picture[1] quantum Hall steps are predicted to disappear for a sufficiently thick electron layer when the cores of extended states from the corresponding Landau levels overlap.

We thank B. I. Halperin for many helpful discussions and J. H. English for help in sample preparation. This work was supported in part by the National Science Foundation under Grants No. DMR-85-08733 and No. DMR-86-14003.

[1]Reviewed in *The Quantum Hall Effect,* edited by R. E. Prange and S. M. Girvin (Springer-Verlag, New York, 1987).

[2]Observed in a thick-layered heterostructure by H. L. Störmer, J. P. Eisenstein, A. C. Gossard, W. Weigmann, and K. Baldwin, Phys. Rev. Lett. **56**, 85 (1986).

[3]Reviewed in B. I. Halperin, Jpn. J. Appl. Phys. **26**, Suppl. 26-3, 1913 (1987).

[4]M. Sundaram, A. C. Gossard, J. H. English, and R. M. Westervelt, Superlattices Microstruct. **4**, 683 (1988).

[5]E. G. Gwinn, P. F. Hopkins, A. J. Rimberg, R. M. Westervelt, M. Sundaram, and A. C. Gossard, in *High Magnetic Fields in Semiconductor Physics II,* edited by G. Landwehr (Springer-Verlag, New York, 1989).

[6]E. G. Gwinn, R. M. Westervelt, P. F. Hopkins, A. J. Rimberg, M. Sundaram, and A. C. Gossard, Superlattices Microstruct. (to be published).

[7]M. Shayegan, T. Sajoto, M. Santos, and C. Silvestre, Appl. Phys. Lett. (to be published).

[8]J. Yoshino, H. Sakaki, and T. Hotta, Surf. Sci. **142**, 326 (1984).

[9]H. L. Störmer, A. C. Gossard, and W. Wiegmann, Solid State Commun. **41**, 707 (1982).